Extended Abstracts of the 2019 International Conference on Solid State Devices and Materials, Nagoya, 2019, pp77-78

Shape optimized nanophotonic devices in 200mm Silicon-On-Insulator platform

Karim Hassan[1], Nicolas Lebbe[1], Laurence Baud[1], Stéphanie Garcia[1], Charles Dapogny[2], Edouard Oudet[2] and Alain Glière[1]

[1] Univ. Grenoble Alpes,
CEA, LETI,
F38000 Grenoble, France
E-mail: karim.hassan@cea.fr
[2] Univ. Grenoble Alpes,
CNRS, Grenoble INP,
LJK, 38000 Grenoble, France

Abstract

We report on the development of Silicon-On-Insulator (SOI) nanophotonic devices designed by shape optimization. Wavelength duplexer is used as a test case to investigate the manufacturability of non-intuitive designs on 200 mm pilot lines. A dedicated fabrication process is used to realize non-Manhattan shapes with a high aspect ratio on SOI. A rather stable and reproducible transmission is found for 6 over 9 dies experimentally measured.

1. Introduction

Shape optimization of nanophotonics devices, also known as inverse design, has received a large attention since the first numerical demonstrations [1, 2]. Such type of design procedure differs from the parametric optimization tools for which quantifiable dimensions are used [3], although genetic algorithm can also be combined with inverse design when the domain is abruptly discretized [4]. Experimental demonstrations of those non-intuitive-shaped devices opens wide prospects for the realization of high density photonics circuits [4,5,6], which must be addressed in the future for chip to chip and intra chip communications, for datacenter and high performance computing application [7]. Nevertheless, the manufacturability of shape optimized designs on large scale tools remains an important point to be investigated [8, 9].

In this contribution, we show the numerical and experimental developments of shape optimized devices based on Hadamard's shape derivative [9], an optimization scheme well established in mechanical engineering. The fabrication is, to the best of our knowledge, realized for the first time onto 200mm wafers using CMOS pilot lines. Preliminary optical characterizations of wavelength divider are shown.

2. Nanophotonic shape optimization

A large number of nanophotonics passive devices based obtained by inverse designed were already proposed in the literature, (mode converter [1, 9], polarization splitters or rotators [4, 10], grating couplers [1], wavelength multiplexers [1, 6, 9]…). Each component can be of interest depending on the application, even though wavelength dividers appears more didactic since the figure of merit relies not only on the power penalty but also on the spectral behavior [1]. We show in the following an example of wavelength duplexers designed for LETI's 200mm platform [11]. The homegrown iterative optimization algorithm, solves Maxwell's equations injecting the fundamental TE at the input port using either finite element method (FEM) or finite difference time domain (FDTD) commercial software's linked to a MATLAB script in a loop [9]. The computational domain is discretized using a 3.6 µm × 3.6 µm × 2 µm wide grid regularly spaced with a mesh of 25 nm in each direction and surrounded by perfectly matched layers. Monitoring the output ports electric field overlap with their respective fundamental modes provides an objective value to be optimized.

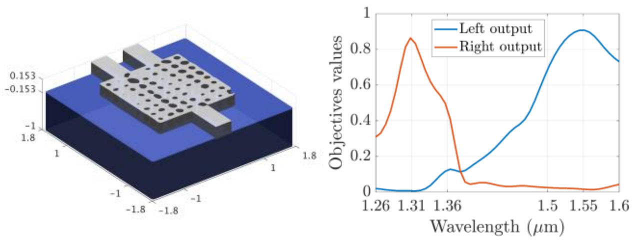

Fig. 1 Schematic 3D view of the optimized compact duplexer and corresponding transmission spectra.

Fig. 1 depicts the optimized duplexer layout and transmission spectra for both outputs, targeting a splitting between O-band and C-band. The sensitivity of conventional photonic devices to manufacturing defects can be usually estimated by taking into account known process variations such as widths variations or etching depth changes. But in the case of non-intuitive shapes, it is not straightforward to make a link with a performance change when the optical field propagates on a random-like structure. In other words, one cannot anticipate how removing or filling any hole of the shape will impact the transmission. Furthermore, the distribution of materials and extremely local aspect ratios makes certainly the process variations unequally distributed. In order to approach roughly the influence of each local element of the shape, one can take a look at the electric filed map norm shown in the Fig. 2 (a) and (b), for O-band and C-band outputs respectively. Since the Hadamard's derivative procedure relies on a local change of shape, one can plot the sensitivity of the domain to a certain change. In the Figs. 2(c)-(d), we calculate the penalty to the O-band and C-band transmission to a 25nm dilatation on the entire structure. This plot highlight a very sensitive region on the bottom left part of the device where changes up to 4% on the transmission can be obtained for a 25nm local dilatation. The most important feature to be noted is the reciprocal changes between the two outputs. When one objective is changes positively by the dilatation, the opposite output is impacted negatively, confirming that the optimization had converged.

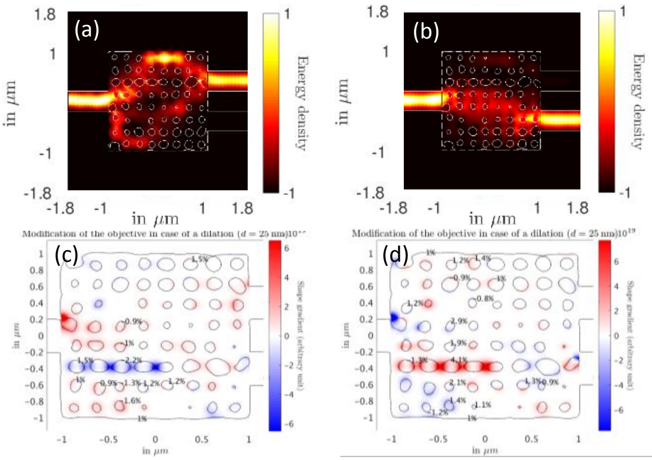

Fig. 2 FDTD Slice of the electric field norm at z = 0 at (a) 1.31µm and (b) 1.55µm; (c), (d) corresponding colormap objective sensitivity plot for changes >0.8%.

3. Fabrication and tests in 200mm SOI substrates

The fabrication process starts using 310nm-thick 200mm SOI wafer with a buried oxide layer of 1µm. After a first level of patterning for the fiber grating couplers, a specific triple layer of resist and hard mask was deposited, consisting on 40nm of a negative tone resist from TOK (OEBR-CAN038) relying on 30 nm of silicon antireflective coating (SiARC) ISX412 and 130nm of Spin on Carbon (SOC) HM8102. An electron-beam lithography equipment available on the 200mm pilot line (VISTEC variable-shape VB6B) was used to pattern small feature size elements down to 18 nm (lines) on the resist. HBr-based reactive-ion etching was used to transfer the waveguides and shapes on the SOI. The ultra-compact wavelength duplexer device descripted above can be seen in Fig. 3 after the lithography (upper left) and after the etching (bottom left). The devices were subsequently tested onto semi-automated fiber to fiber probing stations.

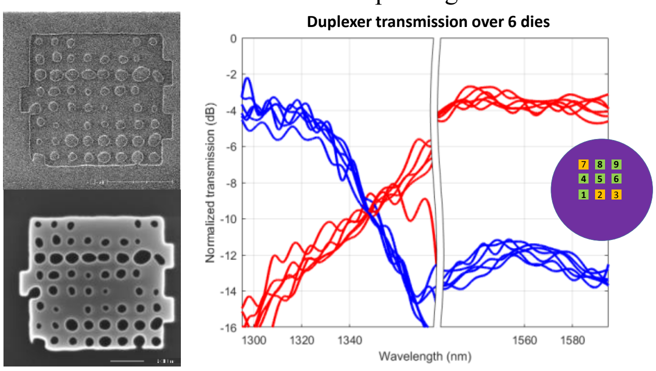

Fig. 3 SEM images after lithography and etching of the shape optimized duplexer and transmission spectra obtained across 6 dies (shown in green on the inset).

The spectrum on 6 over 9 dies of the same wavelength duplexer is plotted in the Fig. 3. While the wavelength scanning was limited by the grating couplers bandwidth on this first wafer, one can see a good reproducibility of the transmission with about -3.5dB and -4dB average insertion losses in the C- and O-band respectively. The 3 others dies tested (not shown here) exhibit different spectral behavior, yet to be investigated by scanning electron microscope (SEM) imaging.

4. Conclusions

In summary, the design, fabrication, and test of shape optimized nanophotonic duplexer was investigated. The calculation reveals the very local sensitivity to shape dilatation, while the experimental measurements shows a rather good reproducibility on 6/9 of the dies in 200mm. Investigation must be pursued on other devices, on robustness optimization, and on DUV immersion lithography.

Acknowledgements

The authors thanks LETI's cleanroom lithography and etching staff for their valuable help, and acknowledge the support of the French national Nano2022 program.

References

[1] Lu, Jesse, and Jelena Vučković. "Nanophotonic computational design." Optics express 21.11 (2013): 13351-13367.

[2] Sigmund, Ole, and Jakob Søndergaard Jensen. "Systematic design of phononic band–gap materials and structures by topology optimization." Philosophical Transactions of the Royal Society of London. Series A: 361.1806 (2003): 1001-1019.

[3] Hassan, Karim, et al. "Robust silicon-on-insulator adiabatic splitter optimized by metamodeling." Applied optics 56.8 (2017): 2047-2052.

[4] Shen, Bing, et al. "An integrated-nanophotonics polarization beamsplitter with 2.4× 2.4 µm 2 footprint." Nature Photonics 9.6 (2015): 378.

[5] Piggott, Alexander Y., et al. "Inverse design and demonstration of a compact and broadband on-chip wavelength demultiplexer." Nature Photonics 9.6 (2015): 374.

[6] Jensen, Jakob Søndergaard, and Ole Sigmund. "Topology optimization for nano‐photonics." Laser & Photonics Reviews 5.2 (2011): 308-321.

[7] Biberman, Aleksandr, and Keren Bergman. "Optical interconnection networks for high-performance computing systems." Reports on Progress in Physics 75.4 (2012): 046402.

[8] Piggott, Alexander Y., et al. "Fabrication-constrained nanophotonic inverse design." Scientific reports 7.1 (2017): 1786.

[9] Lebbe, Nicolas, et al. "Robust shape and topology optimization of nanophotonic devices using the level set method." (2018). ⟨hal-01860882⟩.

[10] Lebbe, Nicolas, Alain Glière, and Karim Hassan. "High-efficiency and broadband photonic polarization rotator based on multi-level shape optimization." Optics letters 44.8 (2019): 1960-1963.

[11] Szelag, B., et al. "Multiple wavelength silicon photonic 200 mm R+ D platform for 25Gb/s and above applications." Silicon Photonics and Photonic Integrated Circuits V. Vol. 9891. International Society for Optics and Photonics, 2016.